

July 05, 2006

Experimental and analytical study of submicrometer particle removal from deep trenches

Kaveh Bakhtari

Northeastern University - National Science Foundation Center for Microcontamination Control

Rasim O. Guldiken

Northeastern University - National Science Foundation Center for Microcontamination Control

Ahmed A. Busnaina

Northeastern University - National Science Foundation Center for Microcontamination Control

Jin-Goo Park

Hanyang University, South Korea - Dept. of Metallurgy and Materials Engineering

Recommended Citation

Bakhtari, Kaveh; Guldiken, Rasim O.; Busnaina, Ahmed A.; and Park, Jin-Goo, "Experimental and analytical study of submicrometer particle removal from deep trenches" (2006). *Center for High-Rate Nanomanufacturing Publications*. Paper 14. <http://hdl.handle.net/2047/d20000925>



Experimental and Analytical Study of Submicrometer Particle Removal from Deep Trenches

Kaveh Bakhtari,^a Rasim O. Guldiken,^a Ahmed A. Busnaina,^{a,*} and Jin-Goo Park^{b,*}

^aNational Science Foundation Center for Microcontamination Control, Northeastern University, Boston, Massachusetts 02115, USA

^bDepartment of Metallurgy and Materials Engineering, Hanyang University, Ansan 426-791, Korea

Particle removal from patterned wafers and trenches presents a tremendous challenge in semiconductor manufacturing. In this paper, the removal of 0.3 and 0.8 μm polystyrene latex (PSL) particles from high-aspect-ratio 500 μm deep trenches is investigated. An experimental, analytical, and computational study of the removal of submicrometer particles at different depths inside the trench is presented. Red fluorescent polystyrene latex (PSL) particles were used to verify particle removal. The particles are counted using scanning fluorescent microscopy. A single-wafer megasonic tank is used for the particle removal. The results show that once a particle is removed from the walls or the bottom of a trench, the vortices and circulation zones keep the particles in the trench for a few minutes before eventually moving the particle out of the trench. The experimental results show that the time required for complete removal of particles from the bottom of the trench takes a much longer time than particles on the surface. This has been also verified and explained by physical modeling of the cleaning process. The removal efficiency and cleaning time are reported at different trench depths.

© 2006 The Electrochemical Society. [DOI: 10.1149/1.2214531] All rights reserved.

Manuscript submitted September 13, 2005; revised manuscript received April 24, 2006. Available electronically July 5, 2006.

The current trend in semiconductor technology toward smaller device features has led to narrower linewidths in integrated circuits (ICs). During the IC fabrication process, trenches and vias have to be cleaned before the next processing step. Contamination during etching, deposition, and other processes is a major concern in IC fabrication because they are responsible for most of the yield losses in semiconductor manufacturing. Although the trench width used in this paper is large for semiconductor applications, it does present valuable information about imaging, counting, and removing nanoscale particles in deep trenches, provided that the particles are much smaller than the trench. The current trench geometry is important to cleaning Head Gimbal Assembly (HGA) at different manufacturing steps in hard disk manufacturing. Megasonic cleaning has been widely used in semiconductor fabrication and other industries for over 30 years and has been found effective in particle removal. Although megasonic cleaning has been used to clean patterned wafers with three-dimensional geometries, the mechanism of megasonic cleaning process for patterned wafer trenches and vias is not well-understood. Prior work that did not involve megasonic cleaning or acoustic streaming reported¹ that sinusoidally forced flow leads to an excellent mixing of the mainstream and the cavity fluid through the mechanism of the destruction and regeneration of the trapped vortex in the cavity (trench or vias). The enhancement of mass transfer in a deep cavity due to external steady channel flow was also investigated.^{2,3} Lin et al.⁴ showed that rinse flow normal to the wafer surface creates orders of magnitudes higher cleaning efficiency than the parallel flow for both steady flow rinse and oscillating flow rinse on wafer surfaces and inside trenches. Nilson and Griffiths⁵ used analytical and numerical methods to solve the equations governing flow and species transport by acoustic streaming within trenchlike features. Deymier et al.⁶ investigated the megasonic cleaning of patterned wafers. They showed that acoustic streaming provides the necessary drag force for particle removal by rolling. Their model did not include the viscous effect which plays a role in the cleaning of trenches. In this paper, we have used viscous flow and modeled the particle–fluid interaction. The removal of 300 and 800 nm particles from deep trenches has been investigated. Experiments and physical modeling was performed to understand the mechanism of detachment of nanoparticles from trenches.

Experimental Procedure and Submicrometer Particle Detection

Removal experiments of 300 and 800 nm polystyrene latex (PSL) fluorescent particles were conducted using 150 mm wafers with six parallel arrays of trenches. The trenches were 112 μm wide and 508 μm deep. The wafers were made of AlTiC (alumina titanium carbide). Particles were deposited into the trench using a nebulizer. Particles are counted at the wafer surface, 100 and 200 μm deep into the trench, and at the bottom of the trench. A Nikon Optiphot 200D microscope equipped with a fluorescent attachment was used to determine the particle count before and after the cleaning process. The microscope is equipped with a standard halogen lamp for optical microscopy, as well as a xenon arc lamp for fluorescent microscopy. Figure 1 illustrates a bright field image of the bottom of the trench. After focusing at the required depth, the microscope was switched to the dark field using the fluorescent attachment to excite the fluorescent particles. The particles then appear as red dots on a black background. Image pro-plus software (vers. 5.1 by MediaCybernetics) was used to count the particles located at a specified location in the trench before and after cleaning. In addition, during the counting of the particles before and after cleaning at the locations specified, special care was taken to prevent counting of possible agglomerated particles. This was done by monitoring the observed particle image aspect ratio.^{7,8}

To verify the nanoparticle counting technique by the fluorescent



Figure 1. Bright field optical image of the bottom of a trench at 500x magnification.

* Electrochemical Society Active Member.

^z E-mail: busnaina@neu.edu

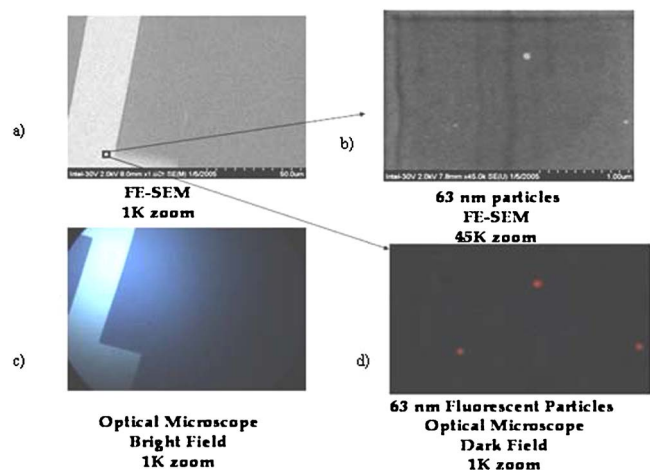


Figure 2. FESEM 63 nm nanoparticle images at (a) 1000x and (b) 45,000x magnification and fluorescent optical images at (c) 1000x at bright field and (d) 1000x at dark field.

microscopy, field emission scanning electron microscope (FESEM) images of nanoparticles were compared to the fluorescent image at the same location. Figure 2 illustrates both FESEM and fluorescent images of a 63 nm fluorescent PSL particles on a wafer. Fluorescent microscopy at 1000x magnification and scanning electron microscopy at 45,000x magnification were used to capture images at the same area on the surface. These FESEM pictures verified that all single particles with a diameter of 63 nm and larger were detectable using the fluorescent microscopy metrology.

A single-wafer megasonic tank at 760 kHz with a maximum power output of 640 W is used in the trench-cleaning experiments. After megasonic cleaning [using deionized (DI) water and 87% of the maximum power], the wafers were spun dry.

Particle Removal Mechanism

There are three possible mechanisms for particle detachment: sliding, rolling, and lifting. In megasonic cleaning, particles are removed by the rolling mechanism. Typically, in the rolling removal mechanism, three forces are involved; the drag force, adhesion force, and double-layer force. Figure 3 shows the forces and the

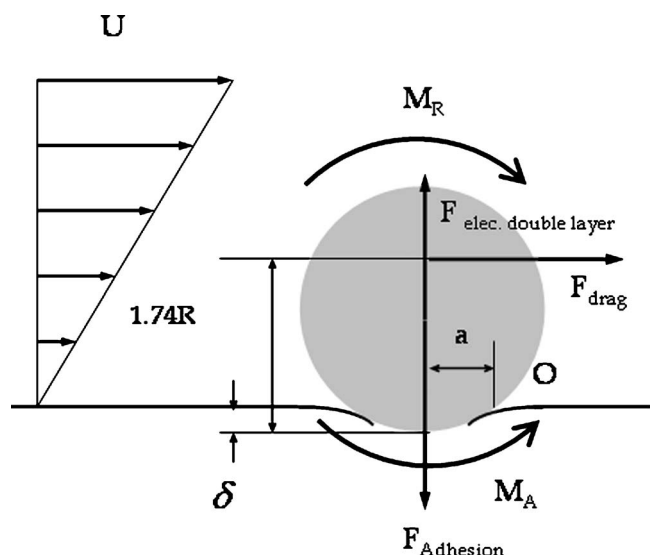


Figure 3. The rolling removal mechanism.

resulting moment of removal, M_R , and the moment of adhesion, M_A , involved in the rolling removal mechanism.

The ratio of the removal moment to the adhesion resisting moment, the moment ratio MR is given by

$$MR = \frac{F_d(1.74R - \delta) + F_{dl}a}{F_a a} \quad [1]$$

where δ is the deformation height of the particle, a is the contact radius between the deformed particle and the surface, F_d is the drag force, F_{dl} is the double layer force, and F_a is the adhesion force. Theoretically, a moment ratio greater than one indicates the particle detachment. This moment ratio model is used to predict the particle detachment from the trench.

The removal moment is the main moment which rolls the particle in the direction of removal. The removal moment is based mainly on the drag force. O'Neill⁹ showed that when a uniform linear shear flow passes a sphere on a wall, the drag force will be

$$F_d = 16\mu d_p u_{dl/2} \quad [2]$$

and the drag moment about the touching point is given by

$$M_d = 1.74RF_d \quad [3]$$

where F_d is the drag force, R is the radius of the particle, μ is the viscosity of the media, d_p is the diameter of the particle, and $u_{dl/2}$ is the velocity of the fluid at the center of the particle. As the equation indicates, the drag moment is a function of the velocity at the center of the particle. For the purpose of the simulation for 300 and 800 nm particles, the maximum velocity at 150 and 400 nm from the trench walls has been used in the moment ratio calculations, respectively. This velocity is determined from the modeling results discussed in the next section. The adhesion moment is the moment resisting the detachment of a particle from a surface. When soft particles are involved, adhesion-induced deformation occurs, resulting in a larger contact area and consequently, a larger adhesion force. Bowling and Mittal¹⁰ gave the total adhesion force, including the component due to the deformation, as

$$F_{ad} = F_{vdW} + F_{vdW-deform} = \frac{AR}{6z_0^2} \left(1 + \frac{a^2}{Rz_0} \right) \quad [4]$$

where A is the Hamaker constant, R is the radius of the spherical particle, z_0 is the separation distance between the particle and the substrate (for smooth surfaces, it is taken as 4 \AA), and a is the contact radius between the deformed particle and the surface. Another force in the moment ratio calculations is the double-layer force, which could be either repulsive or attractive. The PSL particles are negatively charged at neutral pH and the AlTiC wafer is positively charged at the same pH. Therefore in DI water the PSL particles are attracted to the wafer, resulting in an increase in the total adhesion force. However, if the removal force is not sufficient, SC1 could be used as an alternative to DI water. In such a case, the AlTiC surface is negatively charged and the zeta potential interaction force in the particle-wafer system is repulsive, in favor of re-

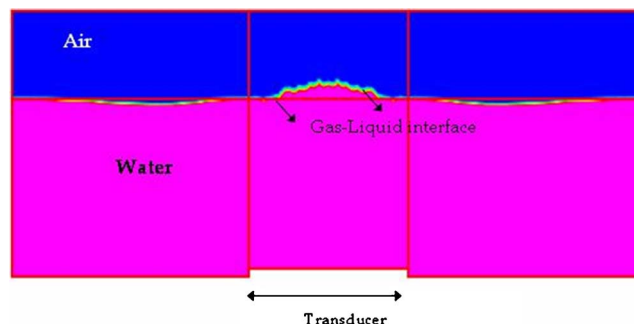


Figure 4. CFD model of the megasonic tank with the liquid-air interface.

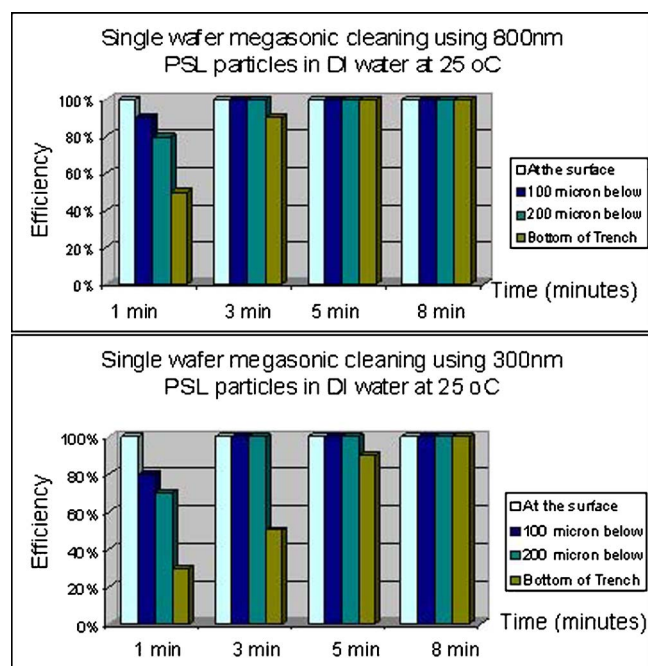


Figure 5. Removal of 300 and 800 nm PSL fluorescent particles in DI water at different depths in the trench as a function of cleaning time.

moving the particle. The following equation, compression approximation,^{11,12} is the appropriate double-layer force expression for the nanoparticle-substrate model and is utilized in the calculations

$$F(D) = \frac{4\pi R\rho_zKT}{\kappa} \left[2Y \ln\left(\frac{B + Y \coth(\kappa D/2)}{1 + Y}\right) - \ln[Y^2 + \cosh(\kappa D) + B \sinh(\kappa D)] + \kappa D \right] \quad [5]$$

where $Y = (y_1 + y_2)/2$, $y = ze\psi/kT$, $B = [1 + Y^2 \csc h^2(\kappa D/2)]^{1/2}$, and κ is the reciprocal of Debye length, which is given by

$$\kappa^2 = \sum_i \frac{\rho_{zi} e^2 z_i^2}{\epsilon \epsilon_0 K T} \quad [6]$$

Physical modeling of the trench cleaning.— A computational fluid dynamics (CFD) model was developed to predict the complete flow field for megasonic cleaning to calculate the acoustic streaming velocity and the removal force exerted on particles located on the trench walls. Figure 4 shows a cross section of a single transducer located at the bottom of the megasonic tank. The transducer was modeled as a moving boundary that moves up and down with specified amplitude at 760 kHz frequency. The gas-liquid interface was also modeled to consider the pressure waves traveling through the media and the surface waves.

Acoustic pressure waves can be considered as attenuated plane waves traveling between two parallel plates. Acoustic streaming velocity at the center of the tank is defined^{13,14} as

$$u = B \left(\frac{h^2}{4} - z_1^2 \right) - K \frac{h^2}{8\mu} \quad [7]$$

where $K = \mu B (2 - 3Z_1^2 + Z_1^3)$, $Z_1 = 2z_1/h$, and $B = (8\Pi^2/3\rho \cdot c^4) I f^2$. In the above equations, ρ is the density of the media, c is the speed of sound in the liquid, μ is the viscosity of the media, I is the intensity of megasonic wave, f is the frequency of the megasonic wave, z_1 the distance between the wall and the center of transducer, and h the distance between the walls of the tank. The velocity field from the megasonic tank model was coupled with a CFD model of a much smaller volume inside the megasonic tank. This smaller volume is a simulation of the liquid inside and immediately outside a trench at the center of the wafer. This simulation enabled us to get a better understanding of the particle detachment and removal from the trench and explain why it takes a relatively long time to completely clean a trench. The results from the simulation are discussed in the next section.

Results and Discussion

The removal efficiency and the time required for 300 and 800 nm PSL particle removal from deep trenches were investigated. The removal efficiency at specified depths within the trench as a function of operating time is shown in Fig. 5. Figure 5 shows that after 1 min of cleaning, complete removal is achieved at the wafer surface near the trench. However, in the trench, the deeper the loca-

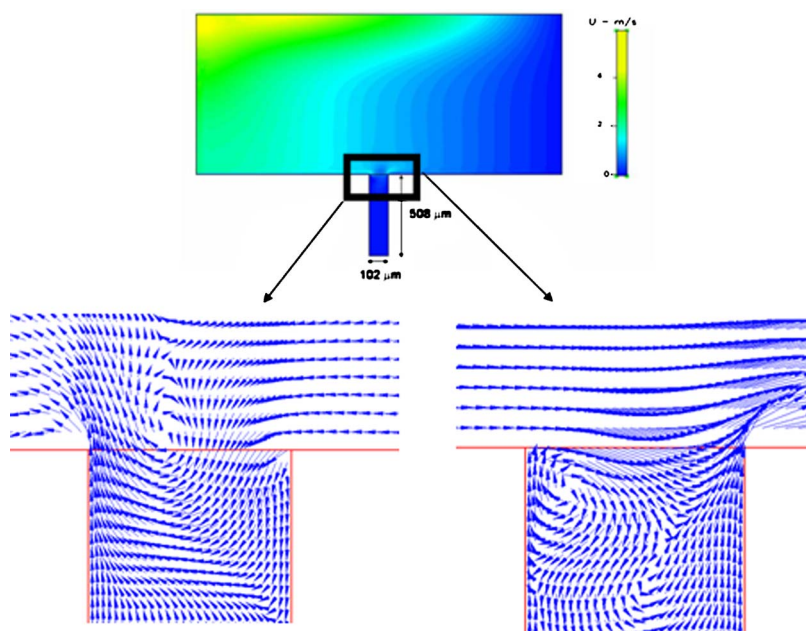


Figure 6. The velocity contour and vector field at two different time steps in the CFD model of the trench.

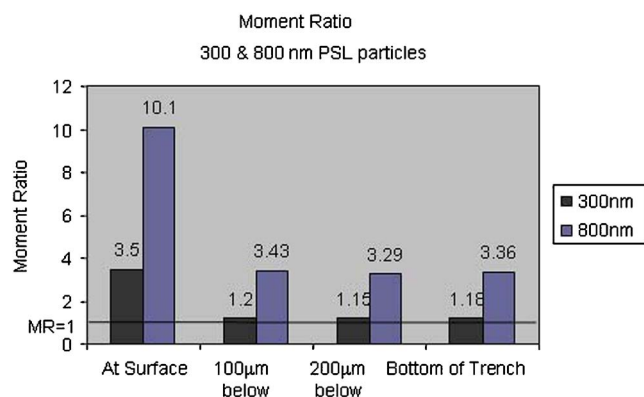


Figure 7. Calculated moment ratio for 300 and 800 nm PSL particles at various locations in a trench.

tion, the lower the removal efficiency is at the same cleaning time. At the bottom of the trench only 30% of the 300 nm particles and 50% of the 800 nm particles are removed after 1 min. Complete removal is achieved after 8 min for 300 nm and 5 min for the 800 nm particles. The shorter removal time observed for the larger particles is due to the larger drag force (due to its larger size).

CFD and the analytical rolling mechanism model, explained in the previous section, were used to understand the effect of cleaning time and depth of trench observed in Fig. 5. Figure 6 illustrates the velocity vector field at two different time steps for the first 100 μm depth within the trench. The velocity vector field shows that the flow is parallel to the sidewalls of the trench. This parallel flow exerts a drag force on the particle (on the sidewall), which induces the particle to roll away from its original location. Figure 6 also shows that the acoustic streaming and pressure fluctuations produce transient vortices inside the trench. Once the particle is detached from the wall, these moving vortices move the particle in an oscillatory motion inside the trench.

The CFD simulations give the velocity field, allowing the drag force on the particle to be calculated. As discussed in the previous section, the moment ratio can be analytically calculated from the drag force, double-layer force, and adhesion force. The moment ratio at different trench depths for the two particle sizes used is shown in Fig. 7. Theoretically, if the moment ratio is greater than one, the removal moment is greater than the adhesion moment and consequently all the particles may be removed. It has been shown experimentally that when the removal moment is equal to one, 80% of the particles are removed. Figure 8 shows experimental results of sub-micrometer silica particle removal as a function of calculated moment ratio on a native oxide silicon surface.¹⁵ Although these results are for silica particles, they demonstrate the relationship between removal efficiency and moment ratio values.

The removal model used here only accounts for Eckart streaming, which is considered as the dominant removal mechanism. There are two other streaming mechanisms: Schlichting streaming and microstreaming. Microstreaming is an important but very difficult to predict mechanism that could contribute 10–30% to the particle removal. Therefore the removal moment used in this model is not the only removal force applied on the nanoparticle and consequently, the theoretical values for the removal efficiency are slightly different from the experimental values, but they follow the same trend. The moment ratio model shows that most of the particles located on the surface of the trench are completely removed.

The simulation also allows us to follow and analyze the particle trajectory after detachment. Once the moment ratio model indicates a particle detachment, a single (300 or 800 nm) particle is released into the flow model at location A in the trench at 100 μm below the surface. The particle trajectory is shown in Fig. 9. After detachment from point A the particle is redeposited twice at locations 1 and 2.

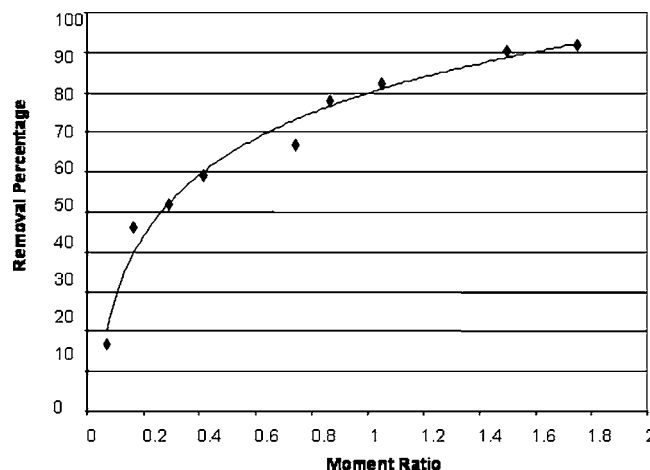


Figure 8. Experimental values for removal efficiency as a function of moment ratio for silica particles.

The particle then moves deep into the trench, more than 300 μm below the surface, to location 3. Afterward, the particle moves to point 4, which is above the original location. The modeling results show the time effect which was observed experimentally and explain the reason for the relatively long cleaning time needed for complete removal. The results show that the particles oscillate up

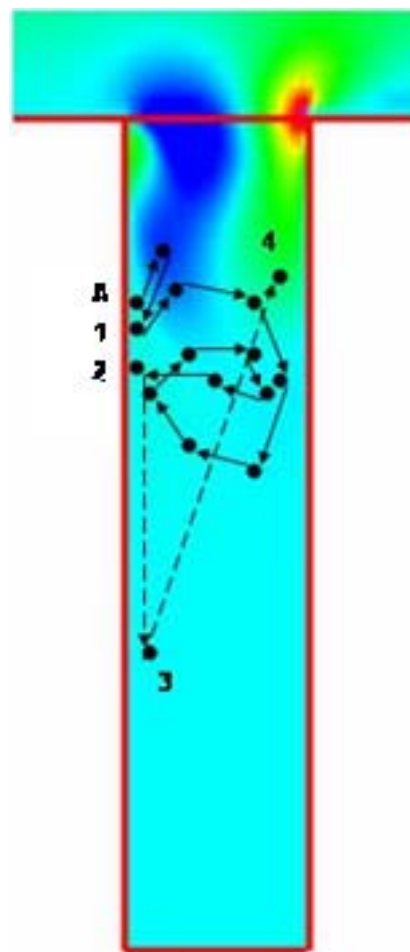


Figure 9. Particle trajectory and redeposition of a particle originally located at 100 μm depth on the wall of a trench.

and down inside the trench for a long time before they eventually leave the trench. The particle trajectory shows that the particle entrapment in the circulation zones, and redeposition on the wall of the trench lead to the long cleaning time. Once the particle is outside the trench it gets swept away by the flow outside the trench.

Conclusions

Complete removal of 300 nm PSL particles from a 500 μm deep trench using 760 kHz oscillatory flow (megasonics) is achieved. After 1 min, complete removal at the wafer surface near the trench is observed. It took 8 min to achieve complete removal of 300 nm particles and 5 min to achieve complete removal of 800 nm particles from the bottom of the trench. The moment ratio model shows that there is a sufficient moment to detach each size particle from the walls and the bottom of the trench. Modeling explained why particles take a long time before they leave the trench. It showed that once detachment takes place, particles undergo an oscillatory motion inside the trench. The particle trajectory shows redeposition of the particles back on the trench walls as well as entrapment inside the circulatory zones within the trench. This leads to a much longer cleaning time (8 min longer for 300 nm particles) compared to particles on the wafer surface. The cleaning trend shown here may be applied to nanoscale trenches, provided that the particles are much smaller than the trench width.

Acknowledgment

This work was supported by the National Science Foundation Center for Microcontamination Control and the Center's industrial members, PCT Systems, Seagate, and DuPont EKC.

Northeastern University assisted in meeting the publication costs of this article.

References

1. J. S. Perkins, K. D. Stephanoff, and B. T. Murray, *IEEE Trans. Compon., Hybrids, Manuf. Technol.*, **12**, 766 (1989).
2. R. C. Alkire, H. Deligianni, and J.-B. Ju, *J. Electrochem. Soc.*, **137**, 818 (1990).
3. J. M. Occhialini and J. J. L. Higdon, *J. Electrochem. Soc.*, **139**, 2845 (1992).
4. H. Lin, A. A. Busnaina, and I. I. Suni, *IEEE Trans. Semicond. Manuf.*, **2002**, 304.
5. R. H. Nilson and S. K. Griffiths, *J. Electrochem. Soc.*, **149**, 286 (2002).
6. P. A. Deymier, J. O. Vasseur, A. Khelif, and S. Raghavan, *J. Appl. Phys.*, **90**, 4211 (2001).
7. O. Guldiken, K. Bakhtari, A. A. Busnaina, and J. Park, *Solid State Phenom.*, **103-104**, 137 (2005).
8. K. Bakhtari, R. Guldiken, A. A. Busnaina and J. Park, The Adhesion Society Proceedings, Mobile, AL, Feb 13-16, 2005, p. 115.
9. M. E. O'Neill, *Chem. Eng. Sci.*, **23**, 1293 (1968).
10. R. A. Bowling and K. L. Mittal, *Detection, Adhesion and Removal*, pp. 129-142, Plenum Press, New York (1988).
11. J. Gregory, *J. Chem. Soc., Faraday Trans. 2*, **69**, 1723 (1973).
12. J. Gregory, *J. Colloid Interface Sci.*, **51**, 44 (1975).
13. W. L. Nyborg, *Physical Acoustics*, Vol. II, Part B, W. P. Mason, Editor, Academic Press, New York (1965).
14. A. A. Busnaina, I. I. Kashkoush, and G. W. Gale, *J. Electrochem. Soc.*, **142**, 2812 (1995).
15. H. Lin, Ph.D. Thesis, Clarkson University, Potsdam, NY (2001).